

# Synthesis and Structural Effect of Multifunctional Photorefractive Polymers Containing Monolithic Chromophores

Jaehoon Hwang, Jiwon Sohn, and Soo Young Park\*

School of Materials Science and Engineering, Seoul National University, ENG445, San 56-1, Shillim-dong, Kwanak-gu, Seoul 151-744, Korea

Received January 26, 2003; Revised Manuscript Received August 11, 2003

**ABSTRACT:** Multifunctional photorefractive polymers bearing five different monolithic chromophores as pendant units were synthesized. Monolithic chromophores are composed of the electron-donating and photoconducting carbazole and the electron-withdrawing nitro group which are connected directly or via different conjugation bridges of azobenzene, stilbene, benzoxazole, and cyanostilbene moiety. Acrylate derivatives of these chromophores were copolymerized with butyl acrylate to give photorefractive polymers with  $T_g$  near room temperature. The structural effects of these monolithic photorefractive chromophores were investigated in terms of the optical nonlinearity, photoconductivity, and photorefractivity of the acrylate copolymers. The opposite direction of asymmetric energy transfer in two-beam coupling measurement indicated that the photorefractive polymers had the different charge-transporting species (hole or electron) for formation of internal space-charge field according to the chromophore structures. The correlation between NLO property and photorefractivity exhibited that the photorefractivities of the obtained polymers were strongly dependent on the NLO property rather than the photoconductivity.

## Introduction

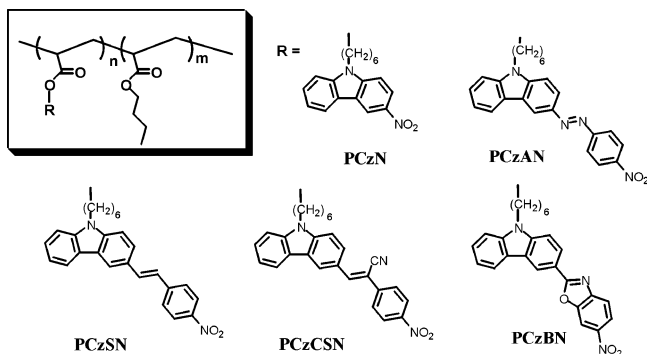
Photorefractive polymers have attracted considerable attention due to their potential applications in the fields of digital holographic data storage, image processing, optical pattern recognition, holographic interferometry, wavelength demultiplexing, and medical imaging.<sup>1,2</sup> The photorefractive effect involves the modulation of the refractive index in an electrooptically active materials due to the internal space-charge field originating from the nonlocal redistribution of photogenerated charge carriers. Therefore, the primary requirements for a material to exhibit the photorefractive are photoconductivity and nonlinear optical (NLO) property in principle.<sup>1,2</sup> There are two different approaches to incorporate these properties into organic materials: one is a multicomponent system,<sup>3–6</sup> and the other is a multifunctional system.<sup>7–10</sup> In the former, photoconductivity and NLO property are provided by the individual structural component, of which the simplest and most successful examples are the composites based on the photoconducting polymer, poly(*N*-vinylcarbazole) (PVK), doped with NLO chromophores and appropriate plasticizer molecules for orientational enhancement effect.<sup>11–13</sup>

Even though many of the reported photorefractive polymers so far are based on this system due to its easier availability and processability, they are always accompanied by the inherent problems, such as the unavoidable phase separation which seriously limits concentration of dopants and also the tradeoff of photoconductivity and NLO property with composition.<sup>1,2</sup> To overcome these problems, fully functionalized materials containing monolithic photorefractive chromophore have been investigated by many research groups,<sup>7–10</sup> although the research in this area is often restricted by the complicated chemical synthesis and unpredictable final properties. In this system, however,

the control of photorefractivity and the molecular design of materials are quite different from that of the multicomponent system, since the required properties for the photorefractive should be provided solely by a single monolithic chromophore. Although the effect of NLO chromophore on the photorefractive performance<sup>12,13</sup> and the guideline for the molecular design of NLO chromophore have been investigated very extensively in multicomponent system,<sup>14,15</sup> the structural effect of monolithic photorefractive chromophore has seldom been studied to date.

To elucidate the structural effect of monolithic chromophore on the photorefractive properties, we synthesized a homologous series of monolithic dipolar chromophores containing carbazole and nitro groups as push–pull elements. Five different conjugation bridges, i.e., direct connection, azobenzene, stilbene, benzoxazole, and cyanostilbene, were incorporated as structure variants of the chromophore units. In our previous work, we have reported the synthesis and properties of potentially photorefractive carbazole-nitro-based polymethacrylate. These multifunctional polymers showed an excellent electrooptic (EO) property and photoconductivity as expected from their structures.<sup>16,17</sup> It was, however, difficult to fabricate 100  $\mu\text{m}$  thick films for photorefractive and/or holographic measurement from these high- $T_g$  polymers due to their brittleness. To overcome this limitation and to impart orientational enhancement, low- $T_g$  photorefractive polyacrylates containing carbazole-nitro-based monolithic chromophore were prepared in this work. Acrylate derivatives of these chromophores were copolymerized with butyl acrylate to give multifunctional photorefractive polymer with glass transition temperature ( $T_g$ ) near room temperature. Scheme 1 shows the chemical structures of the monolithic chromophores and polymers synthesized in this work. Fundamental molecular electronic parameters of the chromophores such as dipole moment, polarizability, anisotropy, and hyperpolarizability were evaluated by semiempirical quantum chemical calcula-

\* Corresponding author: Tel +82-2-880-8327; Fax +82-2-886-8331, +82-2-885-1748; e-mail parksy@plaza.snu.ac.kr.

**Scheme 1. Chemical Structures of Multifunctional Chromophores and Polymers**

tion, and the photorefractive figure-of-merits of chromophores were then estimated by the obtained parameters. The photoconductivity, NLO properties, and the photorefractive properties of these polymers were measured and interpreted in terms of the structure-property correlation in this paper. The nature of the charge carrier transport in the multifunctional photorefractive polymer was also investigated by two-beam coupling and time-of-flight techniques.

### Experimental Section

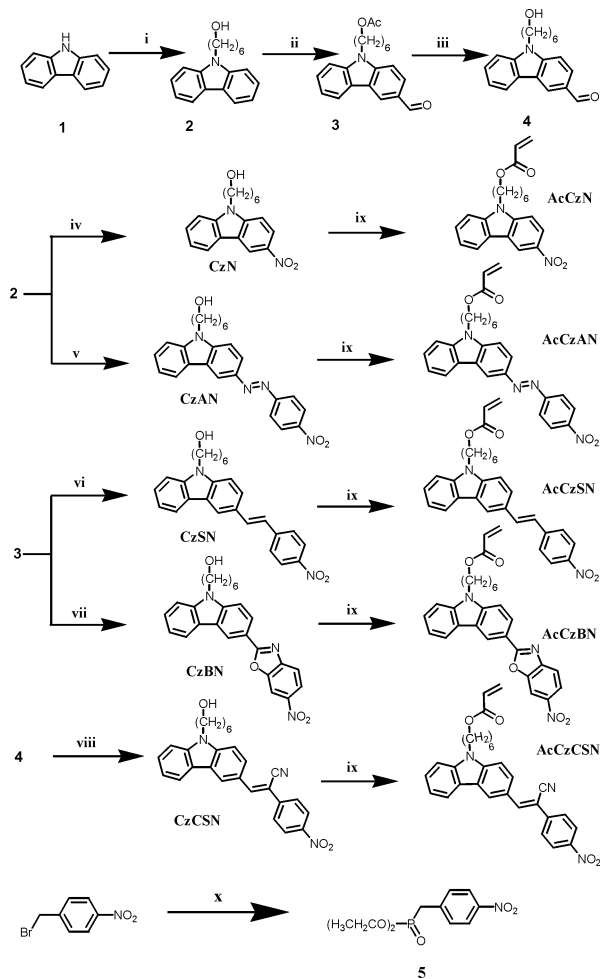
**Materials.** All chemicals were purchased from commercial suppliers and used as received unless otherwise specified. The initiator, 2,2'-azobis(isobutyronitrile) (AIBN) (Aldrich Chemical Co., 98%), and 2-amino-5-nitrophenol (Aldrich Chemical Co., 90%) were recrystallized from methanol and ethanol, respectively. Dichloromethane (Junsei Chemical Co.) used as reaction solvent was dried over  $P_2O_5$ .

**Synthesis of Monomers and Polymers.** Synthetic pathways to the photorefractive chromophores and monomers are outlined in Scheme 2. Synthesis of aldehyde derivatives **3**, **4**, and compound **5** was reported earlier.<sup>7,18</sup>

**6-[3-(4-Nitrocarbazol-9-yl)hexan-1-ol (CzN).** To a magnetically stirred solution of compound **2** (1 g, 4.6 mmol) in dichloromethane (50 mL) was added  $HNO_3$  (0.18 mL, 4.6 mmol) in dichloromethane (20 mL) dropwise at 0 °C. The reaction mixture was stirred at room temperature for overnight. After the solvent was evaporated under reduced pressure, the product was washed with water and recrystallized from ethanol to yield 0.93 g of yellow solid ( $Y = 61\%$ ).  $^1H$  NMR ( $CDCl_3$ ):  $\delta$  9.03 (d, 1H), 8.39 (q, 1H), 8.17 (d, 1H), 7.58 (m, 1H), 7.48 (m, 1H), 7.42 (m, 1H), 7.36 (m, 1H), 4.37 (t, 2H), 3.62 (t, 2H), 1.93 (m, 2H), 1.54 (m, 2H), 1.41 (m, 4H). IR (KBr pellet,  $cm^{-1}$ ): 3304 ( $\nu_{OH}$ ), 1524, and 1316 ( $\nu_{nitro}$ ).

**6-[3-(4-Nitrophenylazo)carbazol-9-yl]hexan-1-ol (CzAN).**<sup>19</sup> 4-Nitroaniline (1.55 g, 11.2 mmol) was dissolved in a solution of concentrated HCl (8 mL) in water (50 mL). The mixture was cooled in an ice bath until temperature was below 4 °C. Then a solution containing sodium nitrite (0.9 g, 13.44 mmol) in water (10 mL) was added slowly to the above solution. The mixture was allowed to stir in the ice bath for 1 h. While the mixture was kept in the ice bath, the phase transfer catalyst, sodium dodecyl sulfate (60 mg), was added. To this solution was added compound **2** (1.5 g, 5.6 mmol) in dichloromethane (50 mL), and then the resultant mixture was stirred vigorously at room temperature for 48 h. The mixture was heated to remove the dichloromethane layer. The red precipitate was filtered, washed with water, and air-dried. The solid was recrystallized from ethanol to yield 1.4 g of red solid ( $Y = 60\%$ ).  $^1H$  NMR ( $CDCl_3$ ):  $\delta$  8.75 (d, 1H), 8.39 (d, 2H), 8.18 (m, 2H), 8.04 (d, 2H), 7.51 (m, 3H), 7.32 (m, 1H), 4.36 (t, 2H), 3.62 (t, 2H), 1.94 (m, 2H), 1.55 (m, 2H), 1.44 (m, 4H). IR (KBr pellet,  $cm^{-1}$ ): 3339 ( $\nu_{OH}$ ), 1535, and 1327 ( $\nu_{nitro}$ ).

**6-[3-[2-(4-Nitrophenyl)vinyl]carbazol-9-yl]hexan-1-ol (CzSN).** To a magnetically stirred solution of **5** (1.14 g, 4.27 mmol) in 10 mL of tetrahydrofuran (THF) was added potas-

**Scheme 2. Synthesis of Multifunctional Chromophores and Monomers**

i = 6-chlorohexanol/NaH, ii = 1) acetic anhydride, 2) DMF/ $POCl_3$ , iii = KOH/EtOH, iv =  $HNO_3$

v = 4-nitroaniline/HCl/ $NaNO_2$ , vi =  $t-BuOK$ / compound **5**

vii = 1) 2-amino-5-nitrophenol, 2) lead(IV) acetate, viii = 4-nitrophenyl acetonitrile,

ix = acryloyl chloride/triethylamine, x = triethyl phosphite

sium *tert*-butoxide (0.67 g, 5.98 mmol) at room temperature. To this solution was added compound **3** (1.5 g, 4.27 mmol), which was dissolved in 10 mL of THF. And then the reaction mixture was heated to 80 °C and stirred for 1 h. To remove the protecting acetyl group, potassium hydroxide (0.47 g, 8.54 mmol) dissolved in ethanol/water (10 mL/10 mL) was added, and this mixture was stirred for another 1 h at 80 °C. After the solution was cooled and the solvent was removed under reduced pressure, the residue was poured onto the ice-cold water and neutralized with 1 N HCl solution. The product was extracted with dichloromethane and washed with plenty of brine and water. After being dried over  $MgSO_4$ , the solvent was removed under reduced pressure. The crude product was purified by column chromatography on silica gel with ethyl acetate/*n*-hexane (vol ratio 1/1) as the eluent to obtain 1 g of orange viscous liquid ( $Y = 56\%$ ).  $^1H$  NMR ( $CDCl_3$ ):  $\delta$  8.28 (d, 1H), 8.23 (d, 2H), 8.15 (t, 1H), 7.68 (m, 3H), 7.52–7.40 (m, 4H), 7.28 (m, 1H), 7.19 (d, 1H,  $J = 16$ ), 4.33 (t, 2H), 3.63 (t, 2H), 1.91 (m, 2H), 1.65 (m, 2H), 1.43 (m, 4H). IR (KBr pellet,  $cm^{-1}$ ): 3416 ( $\nu_{OH}$ ), 1504, and 1343 ( $\nu_{nitro}$ ).

**6-[3-(6-Nitrobenzooxazol-2-yl)carbazol-9-yl]hexan-1-ol (CzBN).** To a boiling solution of compound **2** (3 g, 5.9 mmol) in 1,2-dichlorobenzene (50 mL) was added 2-amino-5-nitrophenol (1.12 g, 6.5 mmol) under magnetic stirring. The reaction mixture was boiled for 2 h, and then the solvent was distilled off in a vacuum. The viscous residue was dissolved in 30 mL of dichloromethane. Under magnetic stirring, lead(IV) acetate (3.16 g, 7.13 mmol) was added in portions. The mixture was

**Table 1. Physical Properties of Multifunctional Photorefractive Polymers**

	feed mole ratio <sup>a</sup>	molar ratio in polymer <sup>b</sup>	yield (%)	$M_n$	PDI	$T_g$ (°C)	$\lambda_{max}$ (nm) <sup>c</sup>	absorption coeff (cm <sup>-1</sup> ) <sup>d</sup>
PCzN	1:3	1:1.9	59	7900	1.9	10	374	15
PCzBN	1:3	1:1.8	50	7700	1.7	24	384	12
PCzSN	1:3	1:1.7	58	6300	2.8	28	414	16
PCzCSN	1:3	1:1.9	47	4000	1.5	24	418	14
PCzAN	1:3	1:2.2	45	5800	1.2	23	434	29

<sup>a</sup> PR monomer: butyl acrylate. <sup>b</sup> Determined by element analysis. <sup>c</sup> Wavelength of absorption maximum estimated in chloroform solution. <sup>d</sup> Determined using polymer films containing 1 wt % of TNF at 633 nm.

stirred at room temperature for 1 h to give a solution with a small amount of suspended solids. After filtration, the solution was washed with water, and the solvent was removed under reduced pressure. This crude product was used in the successive hydrolysis step. It was dissolved in ethanol (48 mL), and potassium hydroxide (0.78 g, 13.9 mmol) dissolved in water (18 mL) was added. After being stirred at reflux for 2 h, the solution was cooled and the solvent was removed under reduced pressure. The residue was poured onto the ice-cold water and neutralized with 1 N HCl solution. Precipitate was filtered and recrystallized from ethanol to yield 0.94 g of yellow solid (37%). <sup>1</sup>H NMR (CDCl<sub>3</sub>):  $\delta$  9.05 (d, 1H), 8.51 (d, 1H), 8.37 (m, 2H), 8.22 (d, 1H), 7.82 (d, 1H), 7.55 (m, 2H), 7.47 (d, 1H), 7.35 (t, 1H), 4.36 (t, 2H), 3.61 (t, 2H), 1.93 (m, 2H), 1.57 (m, 2H), 1.47 (m, 4H). IR (KBr pellet, cm<sup>-1</sup>): 3387 ( $\nu_{OH}$ ), 1506, and 1334 ( $\nu_{nitro}$ ).

**3-[9-(6-Hydroxyhexyl)-9H-carbazol-3-yl]-2-(4-nitrophenyl)acrylonitrile (CzCSN).** To the solution of compound **4** (1.2 g, 4.06 mmol) and 4-nitrophenylacetoneitrile (0.72 g, 4.47 mmol) in 50 mL of ethanol was added piperidine (0.8 mL, 8.12 mmol) at 60 °C. The mixture was stirred at reflux for 2 h and poured into water. The precipitate was collected by filtration and washed with water. The product was purified by recrystallization from ethanol to yield 1.1 g of orange solid ( $Y = 62\%$ ). <sup>1</sup>H NMR (CDCl<sub>3</sub>):  $\delta$  8.71 (d, 1H), 8.31 (d, 2H), 8.18 (t, 2H), 7.88 (m, 3H), 7.57–7.44 (m, 3H), 7.32 (m, 1H), 4.36 (t, 2H), 3.61 (t, 2H), 1.93 (m, 2H), 1.57 (m, 2H), 1.43 (m, 4H). IR (KBr pellet, cm<sup>-1</sup>): 3359 ( $\nu_{OH}$ ), 2198 ( $\nu_{CN}$ ), 1515, and 1343 ( $\nu_{nitro}$ ).

**Acrylic Acid 6-(3-Nitrocarbazol-9-yl)hexyl Ester (AcCzN).** To a magnetically stirred solution of CzN (1.3 g, 4.2 mmol) and triethylamine (1.74 mL, 12.49 mmol) in dichloromethane (20 mL), acryloyl chloride (0.66 mL, 8.3 mmol) was added dropwise at 0 °C. After stirring for 1 h, the resulting solution was allowed to warm to room temperature. After another 1 h, the solution was washed with brine and water and dried over MgSO<sub>4</sub>, and the solvent was removed under reduced pressure. The yellow residue was purified by silica gel column chromatography (ethyl acetate/dichloromethane = 1/15) to yield 1.6 g of yellow solid (70%). <sup>1</sup>H NMR (CDCl<sub>3</sub>):  $\delta$  9.03 (d, 1H), 8.39 (q, 1H), 8.17 (d, 1H), 7.58 (m, 1H), 7.48 (m, 1H), 7.42 (m, 1H), 7.36 (m, 1H), 6.39 (q, 1H), 6.09 (q, 1H), 5.82 (q, 1H), 4.37 (t, 2H), 4.12 (t, 2H), 1.90 (m, 2H), 1.65 (m, 2H), 1.41 (m, 4H). IR (KBr pellet, cm<sup>-1</sup>): 1724 ( $\nu_{C=O}$  of ester), 1504, and 1316 ( $\nu_{nitro}$ ).

**Acrylic Acid 6-[3-(4-Nitrophenylazo)carbazol-9-yl]hexyl Ester (AcCzAN).** AcCzAN was prepared from 0.9 g (2.2 mmol) of CzAN, 0.34 mL (4.3 mmol) of acryloyl chloride, and 0.9 mL (6.5 mmol) of triethylamine by the same procedure as described for AcCzN (0.8 g,  $Y = 77\%$ ). <sup>1</sup>H NMR (CDCl<sub>3</sub>):  $\delta$  8.76 (d, 1H), 8.39 (d, 2H), 8.18 (m, 2H), 8.05 (d, 2H), 7.51 (m, 3H), 7.33 (m, 1H), 6.38 (q, 1H), 6.12 (q, 1H), 5.81 (q, 1H), 4.37 (t, 2H), 4.13 (t, 2H), 1.95 (m, 2H), 1.63 (m, 2H), 1.45 (m, 4H). IR (KBr pellet, cm<sup>-1</sup>): 1718 ( $\nu_{C=O}$  of ester), 1524, and 1339 ( $\nu_{nitro}$ ).

**Acrylic Acid 6-[3-[2-(4-Nitrophenyl)vinyl]carbazol-9-yl]hexyl Ester (AcCzSN).** AcCzSN was prepared from 1.0 g (2.4 mmol) of CzSN, 0.38 mL (4.8 mmol) of acryloyl chloride, and 1.0 mL (7.2 mmol) of triethylamine by the same procedure as described for AcCzN (0.8 g,  $Y = 71\%$ ). <sup>1</sup>H NMR (CDCl<sub>3</sub>):  $\delta$  8.28 (d, 1H), 8.23 (d, 2H), 8.14 (d, 1H), 7.68 (m, 3H), 7.52–7.40 (m, 4H), 7.28 (m, 1H), 7.19 (d, 1H,  $J = 16$ ), 6.38 (q, 1H), 6.12 (q, 1H), 5.80 (q, 1H), 4.33 (t, 2H), 4.12 (t, 2H), 1.91 (m, 2H), 1.65 (m, 2H), 1.43 (m, 4H). IR (KBr pellet, cm<sup>-1</sup>): 1713 ( $\nu_{C=O}$  of ester), 1504, and 1332 ( $\nu_{nitro}$ ).

**Acrylic Acid 6-[3-(6-Nitrobenzooxazol-2-yl)carbazol-9-yl]hexyl Ester (AcCzBN).** AcCzBN was prepared from 0.8 g (1.86 mmol) of CzBN, 0.23 mL (2.8 mmol) of acryloyl chloride, and 0.79 mL (5.6 mmol) of triethylamine by the same procedure as described for AcCzN (0.6 g,  $Y = 67\%$ ). <sup>1</sup>H NMR (CDCl<sub>3</sub>):  $\delta$  9.04 (d, 1H), 8.49 (d, 1H), 8.35 (m, 2H), 8.22 (d, 1H), 7.81 (d, 1H), 7.55 (m, 2H), 7.47 (d, 1H), 7.35 (t, 1H), 6.38 (q, 1H), 6.11 (q, 1H), 5.81 (q, 1H), 4.37 (t, 2H), 4.13 (t, 2H), 1.95 (m, 2H), 1.66 (m, 2H), 1.45 (m, 4H). IR (KBr pellet, cm<sup>-1</sup>): 1715 ( $\nu_{C=O}$  of ester), 1515, and 1343 ( $\nu_{nitro}$ ).

**Acrylic Acid 6-[3-[2-Cyano-2-(4-nitrophenyl)vinyl]carbazol-9-yl]hexyl Ester (AcCzCSN).** AcCzCSN was prepared from 1.1 g (2.5 mmol) of CzCSN, 0.40 mL (5.0 mmol) of acryloyl chloride, and 1.04 mL (7.5 mmol) of triethylamine by the same procedure as described for AcCzN (0.85 g,  $Y = 69\%$ ). <sup>1</sup>H NMR (CDCl<sub>3</sub>):  $\delta$  8.71 (d, 1H), 8.30 (d, 2H), 8.19 (t, 2H), 7.86 (m, 3H), 7.57–7.41 (m, 3H), 7.32 (m, 1H), 6.38 (q, 1H), 6.11 (q, 1H), 5.81 (q, 1H), 4.35 (t, 2H), 4.13 (t, 2H), 1.93 (m, 2H), 1.65 (m, 2H), 1.45 (m, 4H). IR (KBr pellet, cm<sup>-1</sup>): 2198 ( $\nu_{CN}$ ), 1715 ( $\nu_{C=O}$  of ester), 1515, and 1334 ( $\nu_{nitro}$ ).

**Polymerization.** Photorefractive polymers were obtained by free radical copolymerization of monolithic photorefractive monomers and butyl acrylate with feed mole ratio of 1:3. A typical polymerization procedure is as follows: 1.0 g (2.72 mmol) of AcCzN, 1.05 g (8.16 mmol) of butyl acrylate, and 0.089 g (0.55 mmol) of AIBN were dissolved in 10 mL of *N*-methylpyrrolidinone (NMP). The solution was degassed by standard vacuum–freeze–thaw technique. After sealing the degassed ampule, the reaction mixture was heated at 65 °C for 48 h. After cooling, the resulting solution was diluted to twice its original volume with THF and poured into cold methanol to precipitate the polymer PCzN, which was purified by silica gel column chromatography (dichloromethane and THF) (1.2 g, 59%). Compositional mole ratios in obtained polymers were determined by element analysis and summarized in Table 1.

**Characterization.** <sup>1</sup>H NMR spectra were recorded with the use of a JEOL JNM-LA300 spectrometer. IR spectra were measured with KBr pellet or KBr windows on a Bomen FT-IR spectrophotometer. A HP 8452-A spectrophotometer was used for the UV–vis absorption spectra. Gel permeation chromatography (GPC) was performed at a flow rate of 1.0 mL/min in THF at 30 °C with a Waters HPLC component system equipped with five Ultra- $\mu$ -styragel columns (2  $\times$  10<sup>5</sup>, 10<sup>5</sup>, 10<sup>4</sup>, 10<sup>3</sup>, 500 Å), which was calibrated with polystyrene standards. Differential scanning calorimetry (DSC) was carried out under a nitrogen atmosphere at a heating rate of 20 °C/min on a Perkin-Elmer DSC7.

The polymer films with 1 wt % 2,4,7-trinitrofluorenone (TNF) sandwiched between two indium–tin oxide (ITO) covered glasses were prepared by casting from 20 wt % dichloromethane solution. The thickness of the films was maintained at 12  $\mu$ m (for TOF), 25  $\mu$ m (for photoconductivity measurement), and 100  $\mu$ m (for NLO response and photorefractivity measurement) with the polyimide or Teflon spacer.

The dark and photoconductivity of the polymer films were evaluated by measuring a current through the polymer films between ITO glasses using the Keithley 6517 electrometer and 633 nm of He–Ne laser as light source.

Charge carrier mobilities of polymers were measured via the conventional time-of-flight (TOF) technique. The current induced by the laser pulse was transformed to a voltage, which was subsequently amplified and monitored with an oscil-

**Table 2. Calculated Optical Parameters and Figure-of-Merits of Monolithic Chromophores**

	$\mu$ ( $10^{-30}$ C m)	$\Delta\alpha$ ( $10^{-40}$ C m <sup>2</sup> V <sup>-1</sup> )	$\beta$ ( $10^{-50}$ C m <sup>3</sup> V <sup>-2</sup> )	$M$ (g/mol)	$F_{\text{br}}$ ( $10^{-77}$ C <sup>2</sup> m <sup>4</sup> mol V <sup>-2</sup> kg <sup>-1</sup> )	$F_{\text{eo}}$ ( $10^{-77}$ C <sup>2</sup> m <sup>4</sup> mol V <sup>-2</sup> kg <sup>-1</sup> )
CzN	25.12	45.24	2.42	236.23	594.0	2.43
CzBN	25.21	89.66	10.32	343.34	815.4	6.82
CzSN	25.64	101.95	12.52	328.37	1003	8.82
CzCSN-twisted	23.16	84.83	9.69	353.38	632.6	5.76
CzCSN-planar	24.48	98.81	14.99	353.38	823.2	9.34
CzAN	25.66	87.34	9.37	330.34	856.6	6.56

loscope. Then, the mobility was calculated from a transit time  $t_T$  through the relation  $\mu_{h,e} = d^2/(t_T V)$ , where  $d$  is the thickness of the sample and  $V$  is the voltage applied.<sup>20</sup> A nanosecond single pulse of 355 nm light was used to optically generate the charge carriers at the applied voltage of 400 V.

The NLO response was investigated by the ellipsometric technique described in the literature<sup>21,22</sup> to determine the total contribution of the birefringence effect, Pockels effect, and Kerr effect to the overall electric field-induced refractive index changes generated in a low- $T_g$  polymer composite. The voltage applied to the sample was the superposition of a dc component  $V_B$  and a modulated ac component  $V(\Omega) = V_M \sin \Omega$ . In this experiment,  $V_B$  was 4 kV, and  $V_M$  was 600 V whose modulation frequency  $\Omega$  was 1000 Hz, at which the NLO response was governed by both the Pockels effect and birefringence contribution.<sup>23</sup>

Photorefractivity measurements were conducted with a conventional two-beam coupling and degenerated four-wave mixing technique with a 633 nm He-Ne laser. In the two-beam coupling, p-polarized beams with the same intensity of 60.7 mW/cm<sup>2</sup> were intersected in the samples. For the four-wave mixing, two s-polarized beams with the intensity of 60.7 mW/cm<sup>2</sup> were used as writing beams, and a p-polarized reading beam with the intensity of 1.27 mW/cm<sup>2</sup> counter-propagated to one of writing beams. The normal of the sample surface was tilted 60° with respect to the symmetric axis of the two intersected beams, and the external interbeam angle was 11°.

## Results and Discussion

**Synthesis of Chromophores and Polymers.** Monolithic photorefractive chromophores and monomers were successfully synthesized via a synthetic route shown in Scheme 2. CzN and CzAN were obtained by nitration and diazo coupling reaction of compound **2**, respectively. The general procedure of diazotization and diazo coupling are progressed in the aqueous phase, but CzAN was synthesized in the heterogeneous phase with phase transfer catalyst, sodium dodecyl sulfate, since the carbazole derivative **2** is insoluble to aqueous phase.<sup>19</sup> CzSN, CzBN, and CzCSN were obtained by the Wadsworth-Emmons reaction, oxidative ring closing, and the Knoevenagel reaction from aldehyde derivatives **3** and **4**. Their chemical structures were identified by FT-IR and <sup>1</sup>H NMR spectroscopy. In all the chromophores, the stretching vibration of nitro group was observed at ~1500 and ~1300 cm<sup>-1</sup>, and the stretching band of nitrile group in CzCSN was identified at 2198 cm<sup>-1</sup> in FT-IR spectra. The trans structure of the stilbene group in CzSN was also identified by the peaks at 7.2 ppm with the coupling constant of 16 Hz in the <sup>1</sup>H NMR spectrum. Acrylate monomers were easily prepared by the reaction of chromophores and acryloyl chloride, which were confirmed by three vinyl protons at ~6.3, ~6.1, and ~5.8 ppm in <sup>1</sup>H NMR spectra and the absorption peaks of carbonyl group at ~1720 cm<sup>-1</sup> in FT-IR spectra.

To obtain the photorefractive polymers with the low glass transition temperature, acrylate monomers containing these monolithic chromophores were copolymer-

ized with butyl acrylate by free radical polymerization. Because of the higher extent of chain transfer in the radical polymerization of acrylate monomer,<sup>24</sup> the obtained polymers exhibited a relatively lower molecular weight compared to that of the polymethacrylate analogues.<sup>16,17</sup> However, polyacrylates were much softer than polymethacrylate due to the absence of the methyl groups on alternating carbons of the polymer chains.<sup>25</sup> Therefore, all of the obtained polyacrylates showed the glass transition temperature around room temperature, and the transparent thick films with high optical quality could be fabricated for the measurements despite their low molecular weight. Molecular weight and physical properties of obtained polymers are summarized in Table 1.

**Nonlinear Optical Properties and Photoconductivity.** To predict NLO properties of the monolithic photorefractive chromophores, the dipole moment, polarizability anisotropy ( $\Delta\alpha$ ), and hyperpolarizability ( $\beta$ ) were calculated by the semiempirical method, MOPAC 97 with PM3 procedure for geometry optimization in the ground state. For simplicity of calculation, the hydroxyhexyl group in chromophore was substituted by the methyl group.<sup>26</sup> The figure-of-merit of photorefractive chromophore is estimated by the following equation:<sup>1</sup>

$$F = F_{\text{eo}} + F_{\text{br}} = \frac{9\mu\beta}{M} + \frac{2\mu\Delta\alpha}{kTM} \quad (1)$$

where  $M$  is the molecular weight of the chromophore. The first part of the numerator of eq 1 corresponds to the electrooptic (EO) contribution, and the second part corresponds to the birefringence contribution. The calculated molecular electronic parameters ( $\mu$ ,  $\Delta\alpha$ , and  $\beta$ ) and photorefractive figure-of-merits are summarized in Table 2.

The values of  $F_{\text{br}}$  are 2 orders of magnitude larger than those of  $F_{\text{eo}}$ , which means that the contribution of birefringence will play a major role in the refractive index modulation via the orientation enhancement effect, since the glass transition temperatures of the obtained polymers are around room temperature. When a cyano group is introduced into the stilbene, planarity of the conjugated architecture in the optimized geometry is remarkably reduced due to the steric repulsion, and this distortion from planarity causes to reduce the extent of  $\pi$ -orbital conjugation and thus reduced  $\mu$ ,  $\Delta\alpha$ , and  $\beta$  values compared to those of CzSN. However, it is well-known that the twisted structure due to the steric repulsion in isolated gas phase recovers its planar structure when it is solidified, and this planarization leads to extend the effective conjugation length and change the optical properties.<sup>27</sup> In this aspect, we assumed the planar structure of CzCSN and calculated its electric parameters and figure-of-merit value which was comparable to that of the other chromophores.

When the stilbene moiety was replaced by the heteroaromatic benzoxazole group (CzSN  $\rightarrow$  CzBN), the

enhanced aromaticity in the conjugation bridge leads to decrease  $\Delta\alpha$  and  $\beta$ . This can be explained by the fact that additional aromatic delocalization energy limits the excitation, i.e., the intermolecular charge separation and then excitation of the benzoxazole chromophore require a higher energy than that of stilbene chromophore which was confirmed by the blue-shifted absorption maximum ( $\lambda_{\max}$ ) of CzBN compared to that of CzSN. According to the two-level model,  $\Delta\alpha$  and  $\beta$  values decrease as  $\lambda_{\max}$  decreases; therefore, the blue-shifted  $\lambda_{\max}$  of CzBN reduced its figure-of-merit value.<sup>14,26</sup>

It is noted that, in the multifunctional photorefractive materials bearing the monolithic chromophore, the figure-of-merit of photorefractive chromophore could not be considered as the actual degree of photorefractivity, since the formation of space-charge field and the refractive index modulation are influenced by the chromophore structure in this system. In other words, the photoconductive properties of monolithic chromophore, i.e., photogeneration, transport, and trap of charge carrier, were also important factors to determine the photorefractivity. In addition, the birefringence effect originating from the reorientation of chromophore which is the major contribution to figure-of-merit is strongly dependent on the free volume of polymer matrix and  $T_g$ . So in this work, the figure-of-merit was just one of the guidelines to predict the NLO properties of chromophores, and the obtained results confirmed that the monolithic chromophores in this work have sufficient NLO properties compared to the reported NLO chromophores<sup>1</sup> and thus good candidates for the photorefractive molecular materials.

The macroscopic NLO properties of photorefractive polymers were measured by the ellipsometric technique. In this technique, the total electric field applied across the sample is composed of a dc and ac electric field. The dc field induced a permanent chromophore orientation and consequently establishes the noncentrosymmetry required for the second-order NLO properties, and the ac electric field was imposed to probe the magnitude of NLO response. Since the photorefractive polymers studied in this work showed the glass transition around the room temperature, these NLO responses were affected by the combined contribution of birefringence effect and the simple electrooptic effect (Pockels effect) according to the modulated ac voltage. The effective EO coefficient of the samples was estimated by following equation:<sup>21,22</sup>

$$r_{\text{eff}} = \frac{3\lambda I_m}{\pi n^3 I_i V_m} \frac{n\sqrt{n^2 - \sin^2 \theta}}{\sin^2 \theta} \quad (2)$$

where  $I_i$  is half the maximum intensity,  $I_m$  is the modulated intensity,  $n$  is the refractive index of materials,  $V_m$  is the applied ac voltage,  $\lambda$  is the wavelength of laser, and  $\theta$  is the incident angle between laser beam and the sample. As shown in Figure 1, the effective EO coefficients were on the order of PCzAN > PCzCSN > PCzN > PCzSN > PCzBN, although the calculated figure-of-merit values were on the order of CzSN > CzAN > CzCSN(planar) > CzBN > CzN. This different tendency could be ascribed to the different  $T_g$  of polymers, since the motion of chromophore and the contribution of birefringence are strongly dependent on  $T_g$ ; i.e., the higher  $T_g$  of PCzSN and the lower  $T_g$  of PCzN led to decrease and increase the birefringence contribution to NLO response of the samples, respectively.<sup>23</sup>

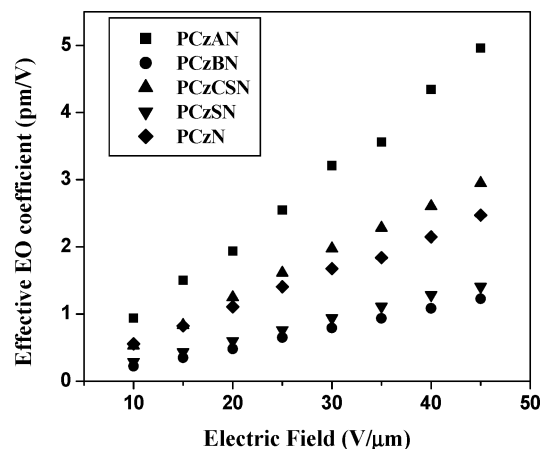


**Figure 1.** Effective EO coefficients as a function of applied field.

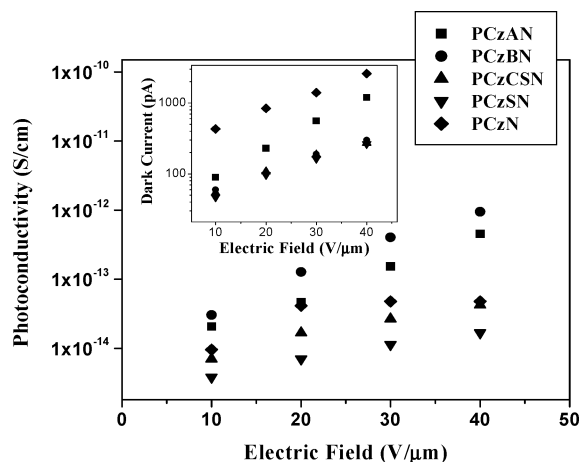


**Figure 2.** Photoconductivity of the multifunctional photorefractive polymers with 1 wt % TNF as a function of applied field. The inset shows the dark currents.

The photoconductive properties of the polymer films were estimated by measuring photocurrent and dark current through the polymer films, and the electric field dependence of the photoconductivity is shown in Figure 2. As expected, PCzBN containing the fused heteroaromatic benzoxazole moiety, which is a well-known photoconductor, as conjugation bridge exhibited the highest photoconductivity,<sup>28</sup> and the strong absorption of PCzAN at 633 nm helped efficient charge carrier generation and led to the higher photoconductivity.

**Photorefractivity.** To determine the photorefractivities of the polymers, the two-beam coupling and four-wave mixing experiments were performed. The two-beam coupling gain was calculated from the asymmetric energy transfer between the two incident beams by the following equation:

$$\Gamma = \frac{1}{L/\cos \theta} [\ln(\gamma_0 \delta) - \ln(\delta + 1 - \gamma_0)] \quad (3)$$

where  $L/\cos \theta$  ( $L$  = sample thickness) is the beam path length,  $\delta$  is the ratio of beam intensities, and  $\gamma_0 = P/P_0$  is the beam coupling ratio ( $P_0$  is the signal beam intensity without the pump beam, and  $P$  is the signal beam intensity with the pump beam).

The calculated gain coefficients are shown in Figure 3. The positive and negative values of gain represent the opposite direction of energy transfer; i.e., in the samples with the positive gain, the energy of beam 2

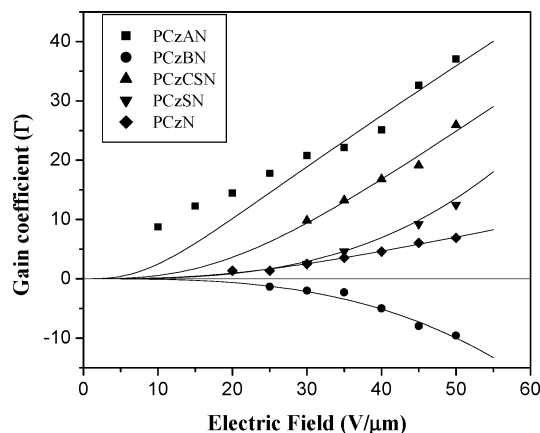


**Figure 3.** Two-beam coupling gain coefficients as a function of applied field. The positive and negative sign of gain coefficients represent the opposite direction of asymmetric energy transfer (see text). Solid lines are guides to the eyes.

**Table 3. Hole and Electron Mobility Measured at 33.3 V/ $\mu\text{m}$  of Applied Electric Field**

	PCzN	PCzBN	PCzSN	PCzCSN	PCzAN
electron mobility, $\mu_e$ ( $10^{-5} \text{ cm}^2/(\text{V s})$ )	1.55	1.46	1.47	1.35	1.49
hole mobility, $\mu_h$ ( $10^{-5} \text{ cm}^2/(\text{V s})$ )	1.49	2.06	1.38	1.19	1.42
$\mu_e - \mu_h$ ( $10^{-5} \text{ cm}^2/(\text{V s})$ )	0.06	-0.5	0.09	0.16	0.07

was transferred to beam 1, while the energy of beam 1 was transferred to beam 2 in the sample with negative gain in our experiment setup. It is well-known that this different direction of energy transfer originates from either the nature of chromophore<sup>29</sup> or the characteristics of charge carrier.<sup>30</sup> First, to investigate the effect of the nature of chromophore, the sign of the field induced refractive index anisotropy was determined by comparing the retardations induced by a Soleil-Babinet compensator in the dc ellipsometric technique as described in ref 29. All of our polymers showed identical signs of birefringence with the compensator modulation, which indicated that the direction of energy transfer was governed solely by the characteristics of charge carriers, i.e., whether the major charge transporting species for the internal space-charge field buildup is hole or electron.<sup>30</sup> To determine which is the major charge transporting species, the electron and hole mobilities of the polymer were measured by the TOF technique, and the obtained results and the difference of electron and hole mobility are summarized in Table 3. In the case of PCzN, PCzSN, PCzAN, and PCzCSN which show the positive gain, the electron mobility was higher than the hole mobility. On the other hand, PCzBN with the negative gain exhibited the faster hole mobility than electron mobility. Consequently, the electron is the major charge transporting species in the materials with the positive gain, and the hole is the major one in the materials with the negative gain in our experiment setup. From these results, it could be said that when the strong electron-withdrawing group was incorporated into the monolithic photorefractive chromophore, the electron mobility exceeds the hole mobility and the electron plays a major role in the formation of internal space-charge field, even though the monolithic chromophores consist of the carbazole moiety which is well-known as the hole transporting material. Refractive index grating induced by hole transporting was observed

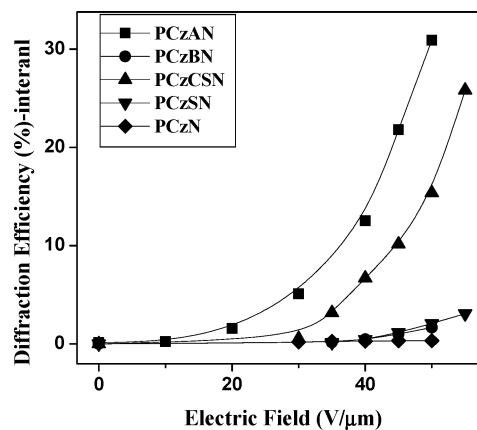


**Figure 4.** Internal diffraction efficiency as a function of applied field. Solid lines are guides to the eyes

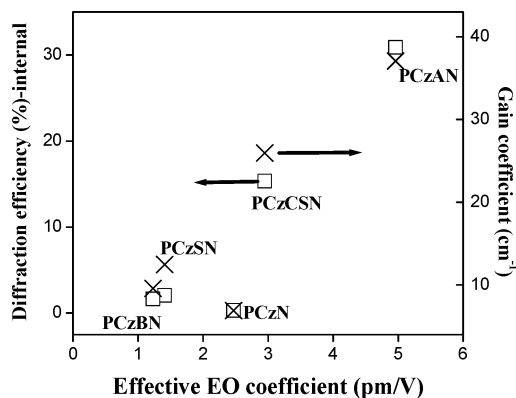


**Figure 5.** Effective EO coefficients (external electric field  $E_0 = 45 \text{ V}/\mu\text{m}$ ) vs diffraction efficiency ( $E_0 = 50 \text{ V}/\mu\text{m}$ ) and gain coefficients ( $E_0 = 50 \text{ V}/\mu\text{m}$ ).

only in PCzBN, since its hole mobility was strongly enhanced due to the fused heteroaromatic benzoxazole moiety,<sup>28</sup> and it was consistent with the result from the photoconductivity measurement. This result means that the nature of the charge carrier transporting for the formation of internal space-charge field in monolithic chromophore system was dependent on the chromophore structure and could be controlled by its modification.

The diffraction efficiency obtained by the following equation is shown in Figure 4:

$$\eta_{\text{int}} = \frac{\text{intensity of the diffracted beam}}{(\text{intensity of the transmitted beam} + \text{intensity of the diffracted beam})} \quad (4)$$

Since the  $\eta_{\text{int}}$  is the ratio of intensity of the diffracted beam to the sum of intensity of the transmitted beam and the diffracted beam, the loss originating from the absorption and reflection in surface of the glass and polymer film was excluded. The photorefractivities, i.e., gain coefficients and diffraction efficiency, were on the order of PCzAN > PCzCSN > PCzN > PCzSN > PCzBN as the NLO response was, while there was no direct correlation between the photorefractivity and the photoconductivity. This correlation between the photorefractivity and the NLO property is shown in Figure 5. In the other words, it could be said that the photorefractivities of the obtained polymers were strongly dependent on the NLO property rather than photoconductivity within the result of our experiments. Deviant

behavior of PCzN from this correlation could be ascribed to the lower  $T_g$  compared to that of the other polymers. It was reported that  $T_g$  below the measurement temperature causes the thermal induced change of the conformational trap, and the charge carriers trapped in such a conformational trap can be released more easily due to the thermal motion. Therefore, the increase of ratio of dark conductivity to photoconductivity leads to reduce internal space-charge field and consequently the decrease of the photorefractivity. It was confirmed by the large dark current of PCzN (inset of Figure 2).<sup>31,32</sup>

## Conclusion

In this work, the multifunctional photorefractive polyacrylates with the monolithic chromophores were synthesized. These photorefractive chromophores consist of the carbazole unit as an electron-donating moiety connected with the electron-withdrawing nitro group via the different conjugation bridges. The correlation between the photorefractivity and the NLO property showed that the photorefractivity of the obtained polymers was strongly dependent on the NLO property rather than photoconductivity within the result of our experiments. The opposite direction of asymmetric energy transfer in the two-beam coupling measurement indicated that the charge transporting species in multifunctional photorefractive polymers could be altered (hole or electron) according to the chromophore structures, which was confirmed by the time-of-flight technique.

**Acknowledgment.** This research was supported in part by CRM-KOSEF. We thank Prof. J.-J. Kim and Mr. Y.-Y. Noh, Kwangju Institute of Science Technology, for the TOF measurement.

## Note Added after ASAP Posting

This article was released ASAP on September 16, 2003. Scheme 2 has been revised. In the Acknowledgment, CRM-KOREF was changed to CRM-KOSEF. The correct version was posted on 09/26/2003.

## References and Notes

- Zilker, S. J. *Chem. Phys. Chem.* **2000**, *1*, 72.
- Wang, Q.; Wang, L.; Yu, L. *Macromol. Rapid Commun.* **2000**, *21*, 723.
- Mecher, E.; Bräuchle, C.; Hörhold, H. H.; Hummelen, J. C.; Meerholz, K. *Phys. Chem. Chem. Phys.* **1999**, *1*, 1749.
- Rahn, M. D.; West, D. P.; Shakos, J. D. *J. Appl. Phys.* **2000**, *87*, 627.
- Mecher, E.; Gallego-Gómez, F.; Tillmann, H.; Hörhold, H. H.; Hummelen, J. C.; Meerholz, K. *Nature (London)* **2002**, *418*, 959.
- Winiarz, J. G.; Zhang, L.; Park, J.; Prasad, P. N. *J. Phys. Chem. B* **2002**, *106*, 967.
- Sohn, J.; Hwang, J.; Park, S. Y.; Lee, G. J. *Jpn. J. Appl. Phys.* **2001**, *40*, 3301.
- Wang, L.; Ng, M.-K.; Yu, L. *Appl. Phys. Lett.* **2001**, *78*, 700.
- Gubler, U.; He, M.; Wright, D.; Roh, Y.; Twieg, R.; Moerner, W. E. *Adv. Mater.* **2002**, *14*, 313.
- Sohn, J.; Hwang, J.; Park, S. Y.; Lee, J.-K.; Lee, J.-H.; Chang, J.-S.; Lee, G. J.; Zhang, B.; Gong, Q. *Appl. Phys. Lett.* **2000**, *77*, 1422.
- Park, S.-H.; Ogino, K.; Sato, H. *Synth. Met.* **2000**, *113*, 135.
- Díaz-García, M. A.; Wright, D.; Caspersen, J. D.; Smith, B.; Glazer, E.; Moerner, W. E.; Sukhomlinova, L. I.; Twieg, R. J. *Chem. Mater.* **1999**, *11*, 1784.
- Hendrickx, E.; Zhang, Y.; Ferrio, K. B.; Herlocker, J. A.; Anderson, J.; Armstrong, N. R.; Mash, E. A.; Persoons, A. P.; Peyghambarian, N.; Kippelen, B. *J. Mater. Chem.* **1999**, *9*, 2251.
- Beckmann, S.; Eitzbach, K.-H.; Krämer, P.; Lukaszuk, K.; Matschiner, R.; Schmidt, A. J.; Schuhmacher, P.; Sens, R.; Seybold, G.; Wormann, R.; Würthner, F. *Adv. Mater.* **1999**, *11*, 536.
- Würthner, F.; Wormann, R.; Meerholz, K. *Chem. Phys. Chem.* **2002**, *3*, 17.
- Kim, D. W.; Hong, S. I.; Park, S. Y.; Kim, N. *Bull. Korean Chem. Soc.* **1997**, *18*, 198.
- Kim, D. W.; Moon, H.; Park, S. Y.; Hong, S. I. *React. Funct. Polym.* **1999**, *42*, 73.
- Moon, H.; Hwang, J.; Kim, N.; Park, S. Y. *Macromolecules* **2000**, *33*, 5116.
- Ho, M.; Barrett, C.; Peterson, J.; Esteghamatian, M.; Natan-sohn, A.; Rochon, P. *Macromolecules* **1996**, *29*, 4613.
- Ostroverkhova, O.; Singer, K. D. *J. Appl. Phys.* **2002**, *92*, 1727.
- Kippelen, B.; Sandalphon; Meerholz, K.; Peyghambarian, N. *Appl. Phys. Lett.* **1996**, *68*, 1748.
- Teng, C. C.; Man, H. T. *Appl. Phys. Lett.* **1990**, *56*, 1734.
- Hwang, J.; Seo, J.; Sohn, J.; Park, S. Y. *Opt. Mater.* **2003**, *21*, 359.
- Moad, G.; Solomon, D. H. *Chemistry of Free Radical Polymerization*; Pergamon: Oxford, 1995; pp 251–257.
- Odian, G. *Principle of Polymerization*, 2nd ed.; Wiley-Interscience: New York, 1991; p 311.
- Kim, S.; Moon, H.; Hwang, J.; Sohn, J.; Seo, J.; Park, S. Y.; Kang, T. I.; Cho, B. R. *Chem. Phys.* **2000**, *256*, 289.
- An, B.-K.; Kwon, S.-K.; Jung, S.-D.; Park, S. Y. *J. Am. Chem. Soc.* **2002**, *124*, 14410.
- Kim, S.; Park, S. Y. *Macromolecules* **2001**, *34*, 3947.
- Aiello, I.; Dattilo, D.; Ghedini, M.; Bruno, A.; Termine, R.; Golemme, A. *Adv. Mater.* **2002**, *14*, 1233.
- Okamoto, K.; Nomura, T.; Park, S.-H.; Ogino, K.; Sato, H. *Chem. Mater.* **1999**, *11*, 3279.
- Bittner, R.; Däubler, T. K.; Neher, D.; Meerholz, K. *Adv. Mater.* **1999**, *11*, 123.
- Swedek, B.; Cheng, N.; Cui, Y.; Zieba, J.; Winiarz, J.; Prasad, P. N. *J. Appl. Phys.* **1997**, *82*, 5923.

MA034104G